Ocean Waves Measurement and Analysis, Fifth International Symposium WAVES 2005, 3rd-7th, July, 2005. Madrid, Spain
Paper number: 166

EXPERIMENTAL VALIDATION OF A COUPLED BEM-NAVIER-STOKES MODEL FOR SOLITARY WAVE SHOALING AND BREAKING

D. Drevard[1],R. Marcer [2], S.T. Grilli[3], M. ASCE, P. Fraunié[1] and V. Rey[1]

Abstract: This paper studies the shoaling, breaking, and post-breaking of solitary waves, using a numerical model based on the coupling between a higher-order Boundary Element Method (BEM) and a Volume Of Fluids (VOF) solution of Navier-Stokes (NS) equations, having an improved interface tracking algorithm (SL-VOF). In the coupled model, the BEM solution is used to initialize the VOF-NS computations. The paper reports on the experimental validation of numerical simulations, for two-dimensional (2D) breaking waves. Two different applications are considered. The first one is the case of the breaking of a solitary wave over a step, which was experimentally tested by Yasuda et al. (1997). The second case is that of the shoaling and breaking of solitary waves on a constant mild slope. Results are compared to experiments performed at ESIM (Marseille, France).

INTRODUCTION

Breaking waves on beaches and over ocean bottom discontinuities, constitute one of the most energetic events in the coastal environment. A better understanding and modeling of the kinematics of breaking waves is of prime importance for coastal engineering problems. Significant progress in both the physical understanding and the numerical modeling of wave breaking have been made in recent years. In particular, due to the increasing power of modern computers, direct Computational Fluid Dynamics (CFD) simulations of wave breaking can now be carried out. Proper experimental validation of such simulations, however, is still a necessary step both for model development and in the analysis of model predictions.

Computational methods used to simulate wave breaking can be divided into two groups. The first one consists in following the free surface motion as a function of time, using an adapted or deformed grid. In such an approach, models based on fully nonlinear potential flow equations, usually solved with a Boundary Element Method (BEM), have proved very accurate and efficient, particularly for simulating wave overturning over constant depth (e.g.,

[1]Laboratoire de Sondages Electromagnétiques de l'Environnement Terrestre, Université de Toulon et du Var - BP 132, 83957 La Garde cedex, France, deborah.drevard@lseet.univ-tln.fr
[2]Principia Z.I. Athélia 13705 La Ciotat Cedex, France
[3]Department of Ocean Engineering, University of Rhode Island, Narragansett, RI 02882, USA; grilli@oce.uri.edu

Longuet-Higgins and Cokelet, 1976, 1978) or wave transformations over an arbitrary bottom topography, up to overturning (e.g., Grilli et al. 1992, 1994, 1996, 1997). Such models, however, are unable to deal with interface reconnections and large deformations occurring during wave breaking, for which potential theory is invalid. In the second group of models, the solution is based on the computation of the interface motion in a fixed grid, using the full Navier-Stokes (NS) equations, which allows to simulate the full wave breaking. In this group, the Volume Of Fluids (VOF) method, first developed by Hirt and Nichols (1981), is likely one of the better adapted models to treat complex interface shapes, such as occurs during wave breaking. A key problem of the latter models, however, is their high computational cost as compared to BEM models. To combine the advantages of both types of models, a coupled approach was proposed in earlier work, in which pre-breaking waves are computed with the BEM method, and breaking and post-breaking waves are computed using the VOF model (Guignard et al., 1999; Lachaume et al., 1993; Biausser et al., 2004a,b).

Although three-dimensional problems have been solved, in this study, the coupling of BEM and VOF-NS models is performed in two dimensions (2D). The BEM solution, obtained with Grilli et al.'s (1996) and Grilli's (1997) model, is used as an initial solution for the VOF-NS model computations. The BEM model equations are summarized in the first section. The second section deals with the VOF-NS model. Then, two applications of breaking wave simulations are presented, with a comparison with experiments.

BEM MODEL

Mathematical Formulation

Equations for fully nonlinear potential flows with a free surface are listed below. The velocity potential $\phi(x,t)$ is introduced to describe inviscid irrotational 2D flows, in Cartesian coordinates (x,y), with y the vertical upward direction ($y=0$ at the undisturbed free surface), and the fluid velocity is expressed as $\mathbf{u}=\nabla\phi$. Continuity equation in the fluid domain $\Omega(t)$ with boundary $\Gamma(t)$ is a Laplace's equation for the potential, $\nabla^2\phi=0$. Using the free space Green's function, $G(\mathbf{x},\mathbf{x}_l)=-(1/2\pi)\log|\mathbf{x}-\mathbf{x}_l|$, Green's second identity transforms the latter equation into the Boundary Integral Equation (BIE),

$$\alpha(\mathbf{x}_l)\phi(\mathbf{x}_l)=\int_{\Gamma(\mathbf{x})}\left\{\frac{\partial\phi}{\partial n}(\mathbf{x})G(\mathbf{x},\mathbf{x}_l)-\phi(\mathbf{x})\frac{\partial G(\mathbf{x},\mathbf{x}_l)}{\partial n}\right\}\mathrm{d}\Gamma(\mathbf{x}) \tag{1}$$

The boundary is divided into various parts, over which different boundary conditions are specified. On the free surface, ϕ satisfies the nonlinear kinematic and dynamic conditions,

$$\frac{D\mathbf{r}}{Dt}=\left(\frac{\partial}{\partial t}+\mathbf{u}\cdot\nabla\right)\mathbf{r}=\mathbf{u}=\nabla\phi \quad ; \quad \frac{D\phi}{Dt}=-g\,y+\frac{1}{2}\nabla\phi\cdot\nabla\phi-\frac{p_a}{\rho} \tag{2}$$

respectively, with $\mathbf{r}$ the position vector of a fluid particle on the free surface, g the gravitational acceleration, p_a the pressure at the free surface and ρ the fluid density. On the bottom and other fixed parts of the boundary, a no-flow condition is prescribed as, $\frac{\partial\phi}{\partial n}=0$.

Numerical method for the BEM Model

A Lagrangian second-order explicit scheme, based on Taylor series expansions, is used for the time updating of the position $\mathbf{r}$ and velocity potential ϕ on the free surface. First-order coefficients are given by Eqs. (2) and second-order coefficients, by the Lagrangian

time derivative of these. A higher-order BEM is used for the numerical solution of BIE (1) for ϕ, and a similar BIE for $\partial\phi/\partial t$ (Grilli and Subramanya, 1996). The boundary is discretized into collocation nodes, defining two-dimensional elements for the local interpolation of the solution in between these nodes. Within each element, the boundary geometry and field variables are interpolated using cubic polynomial shape functions (4-node "sliding" elements are defined, of which only the middle two nodes are used). The discretized BIEs are evaluated for each collocation node by numerical integration. A special treatment is applied for weakly singular integrals. The linear algebraic system resulting from the discretization of the BIE is in general dense and non-symmetric; for 2D problems, a direct solution based on Kaletsky's method is used (for 3D problems, not reported here, a generalized minimal residual algorithm with preconditioning is used to solve the algebraic system). Accuracy is increased in regions of high variability by redistributing nodes using a regridding technique based on the BEM shape functions.

VOF-NS MODEL

Navier-Stokes/VOF Formulation

We consider a moving interface defined as the limit between two incompressible viscous fluids of different densities. The problem is to compute the pressure and velocity fields in the denser fluid and to track the interface motion.

The interface and its motion are described by an original method, called SL-VOF (Guignard et al., 2001 for 2D-flows; Biausser et al., 2004a for 3D-flows), which combines the VOF method (Hirt and Nichols, 1981) with a Piecewise Linear Interface Calculation (PLIC) (Li, 1995). The position of the interface is thus calculated in each cell by way of a discrete function C whose value, between 0 and 1, denotes the fraction of the cell space filled with the denser fluid (VOF concept). The original SOLA-VOF method (Hirt and Nichols, 1981), which is based on the resolution of a conservation equation for the VOF function, assumes that the interface is parallel to the grid sides. Hence, the resolution of this method is quite low, particularly for complex interfaces such as found in breaking waves. By contrast, the SL-VOF method allows for the interface to be represented by oblique segments (plans in 3D) of any orientation (PLIC concept). Moreover, due to the Lagrangian description in the PLIC method, there is no need to solve a conservation equation for the VOF function. Thus, the main advantages of this method, as compared to the original VOF method, are a higher accuracy of the interface description and the capacity to use larger time steps, resulting in a significant gain in computational time.

Numerical method for the VOF-NS Model

Time integration is based on a fully implicit second-order finite difference scheme. The solution of the nonlinear system is based on the "pseudo-compressibility method" (Viviand, 1980; De Jouëtte et al., 1991). In this method, a time-like variable τ, called pseudo-time, is introduced in the equations, creating an additional pseudo-unsteady term, which involves a new unknown $\tilde{\rho}$, called pseudo-density (constrained to remain positive). The fluid pressure is calculated as a function of $\tilde{\rho}$. The choice of an optimal pseudo-state equation is discussed in Viviand (1995). The system of equations is integrated step-by-step in pseudo-time, with an explicit five step Runge-Kunta scheme.

Coupling BEM-VOF-NS models

The VOF-NS model can simulate wave propagation, breaking, and post-breaking over slopes, or other complex bottom topography. However, to be accurate, this model requires a sufficiently fine numerical grid, as compared to the scale of variation of physical phenomena to be simulated. This makes computations over large domains prohibitive. Another limitation is that the VOF method may induce unwanted numerical dissipation, when applied to the simulation of wave propagation over a long distance, leading to non-physical loss of wave energy.

As discussed in the introduction, the coupled BEM-VOF-NS model approach allows to overcome these limitations. Thus, we use the very accurate and efficient BEM model to simulate wave propagation over constant depth and in the shoaling zone, and couple it to the VOF-NS model to simulate waves in the breaking region. Here, according to the method referred to as weak coupling (e.g., Guignard et al., 1999; Lachaume et al., 2003), model coupling is carried out by specifying the internal values of the dynamic pressure and velocity field computed with the BEM model over the VOF grid. The dynamic pressure field is obtained from Bernoulli equation, which requires also calculating the time derivative of the potential. The interior control points of the BEM correspond to the centers of the VOF cells, so that it is easy to transfer velocity and pressure values to the NS mesh. The VOF field is finally computed by interpolation, based on the shape of the BEM free surface. Note that with this methodology, no VOF-NS results are fed back into the BEM model (this would represent a so-called strong coupling situation).

Various types of incident waves can be specified in the BEM model (Grilli and Horrillo, 1997). For solitary waves, Tanaka's (1986) algorithm has been implemented to compute numerically exact free surface shape, potential, and normal derivative of the potential at initial time (Grilli and Subramanya, 1996).

APPLICATIONS

Breaking of a solitary wave over a step

The propagation of a solitary wave over a step or other submerged breakwaters, or reefs, has been the object of many studies, both experimental and numerical (e.g., Grilli et al., 1992, 1997; Yasuda et al., 1997). Solitary waves are a good model of extreme long waves, such as tsunamis, but also are both a simple and a good approximation for long nonlinear shallow water waves.

Here, the domain configuration of Yasuda et al.'s (1997) experiments is used to study solitary wave propagation over a submerged step, in both the BEM and the VOF-NS models (Fig. 1). This case was also recently used by Helluy et al. (2005), as an experimental benchmark, to compare results of several numerical models. Experimental data include wave elevation measured at 3 wave gages P1, P2, P3, and visualizations of breaking wave shapes. The initial condition is specified as a numerically exact solitary wave, with its maximum elevation located at $x = 0$. The initial velocity and pressure fields for this wave are generated using the BEM model and used, together with wave shape, as an initial condition in the VOF-NS model. The wave height is $H = 0.131$ m over constant depth $h_1 = 0.31$ m, thus $H/h_1 = 0.423$. The wave propagates with an initial phase velocity of $c_o = 1.18\sqrt{gh_1} = 2.06$ m/s. VOF computations are made in a rectangular domain, 8 meters long ($x \in [-2, 6]$) and

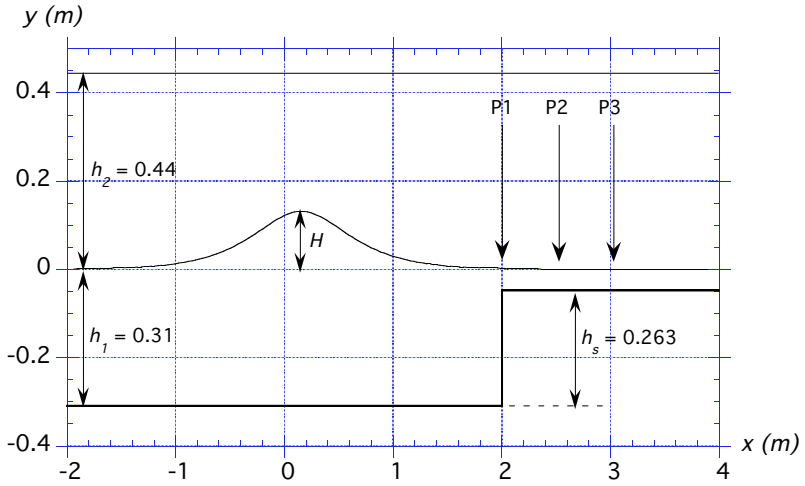

Fig. 1. Configuration of Yasuda's (1997) experiments.

0.75 meters high ($y \in [-0.31, 0.44]$), using 1000×200 computational cells. A rectangular step of height $h_s = 0.26$ m is modeled on the bottom, 4 meters from the leftward boundary.

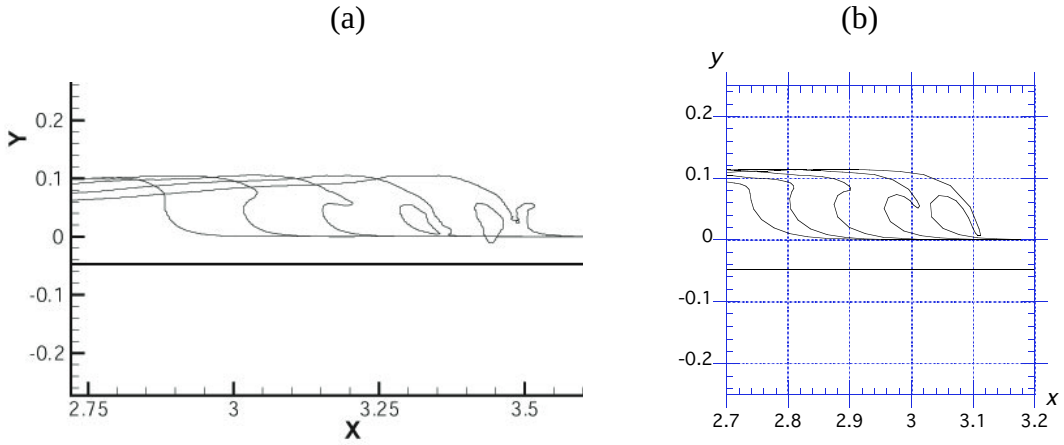

Fig. 2. Evolution of the solitary wave over the step until splash-up/overturning: (a) VOF-NS; (b) BEM (last profile is at t = 1.35 s).

At the beginning of computations, the wave propagates on a flat bottom without deformation in both models. When it reaches the step, part of the wave is reflected and part of the wave is transmitted over the step (Fig. 2). The front of the transmitted wave steepens up and a jet starts forming at its crest, due to the reduced wave celerity in the shallower depth $h_1 - h_s = 0.047$ m. Then, the wave overturns and break. The jet impacts at about 3.35 m from the initial condition in the VOF model, and 3.12 m in the BEM model. Fig. 2 shows that both models accurately describe those phases. The inviscid BEM model does not include any dissipation due to flow separation at the step and, hence, computes higher transmitted waves, which evolve faster. The last overturning profile computed in the BEM model, slightly before jet impact, is at $t = 1.35$ s. The VOF-NS model accurately simulates both jet impact and post-breaking phases during which a secondary jet ejection occurs. This phenomenon is usually referred to as splash-up.

Surface elevations computed in both models are compared with Yasuda et al.'s (1997)

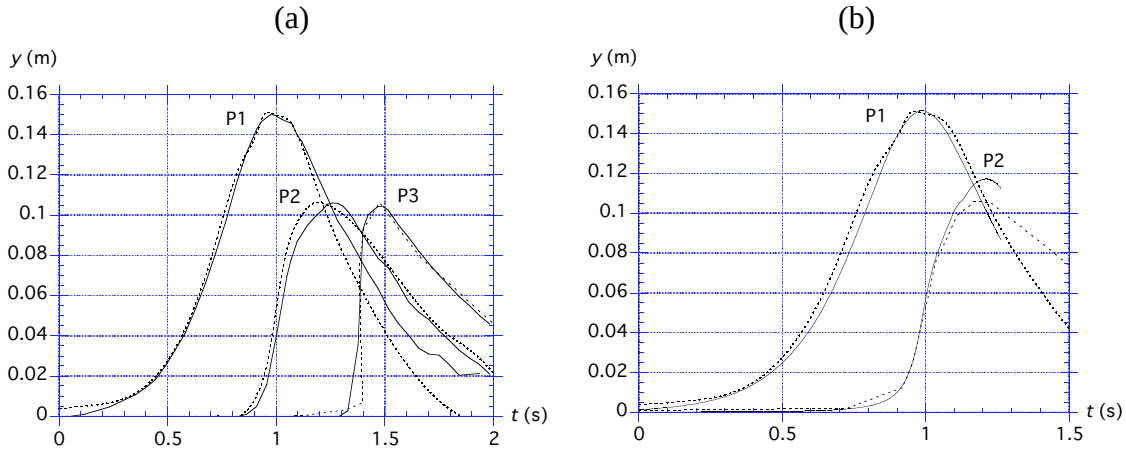

Fig. 3. Comparison of computed surface elevations (——) with Yasuda et al.'s (1997) experiments (- - - - -) at gages gages P1 (x=2 m), P2 (x=2.52 m), and P3 (x=3.02 m) (Fig. 1): (a) VOF-NS; (b) BEM.

experimental data, at three different gage locations (Figs. 1 and 3). BEM computations are interrupted at $t = 1.35$ s, when jet impact occurs. The first gage, P1, is located at the step, where we see that waves computed in both models agree well with experiments. At this instant, the solitary wave is not yet significantly affected by the effect of the step and it still has a shape close to its initial shape, except for a slight increase in amplitude due to reflection. For the two following gages, P2 and P3, located over the step, the wave begins and then intensifies its deformation. The front of the wave steepens up, reaching a vertical slope; then, a jet appears at the crest, initiating wave overturning. The comparison of measurements at gages shows that wave elevations computed in the VOF-NS model are still in good agreement with experimental results. In the BEM model, however, wave elevations are slightly overpredicted near the crest. This is due to the lack of energy dissipation at the step in the BEM model.

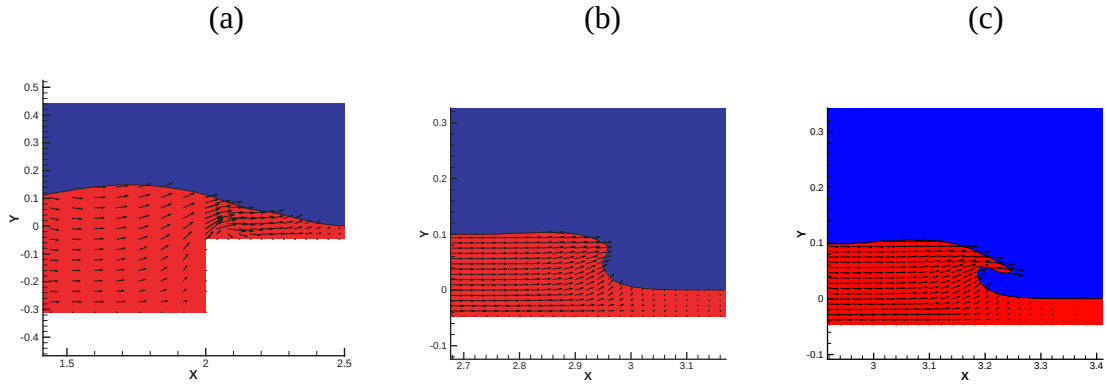

Fig. 4. Velocity field in VOF-NS model, for time t= (a) 0.35 s, (b) 0.56 s, and (c) 0.63 s.

Figure 4 shows velocity fields computed in the VOF-NS model, for three different times. At $t = 0.35$ s, flow velocities are seen to intensify in the shallower water at the beginning of the step, as compared to their values in front of the step, due to flow convergence. The latter phenomenon also causes strong vertical flow velocities. Flow separation is also visible at the step. Later on ($t = 0.56$ s), transfer of the wave crest occurs from the deeper to the shallower region, and this phenomenon causes increased deformation of the wave crest,

which steepens up. Flow convergence towards the crest follows and causes the wave profile to become even more asymmetric. The wave at this stage appears as having two regions: (i) a uniform flow over depth in the back, and (ii) a flow convergence at the crest, in the front. At the breaking point, when the wave front slope is vertical, the wave starts overturning and the crest plunges forward. From this instant onward, flow velocities in the jet intensify and are directed horizontally and slightly downwards ($t = 0.63$ s). The computed velocity field is similar to that observed in a plunging wave over a slope (Grilli et al., 2004).

Breaking of a solitary wave over a sloping bottom

In this application, the VOF-NS model is validated based on experiments performed in the laboratory of the Ecole Supérieure d'Ingénieurs de Marseille (ESIM). This work was carried out within the framework of the program PATOM ("Programme Atmosphére et Océan á Multi-échelles") of the French CNRS. Details of ESIM's laboratory experiments can be found in Kimmoun et al. (2004), as well as Grilli et al. (2004). Solitary waves were generated in a transparent wavetank, using a flap wavemaker whose axis of rotation was located below the tank bottom. The law of motion of the wavemaker was defined analytically such as to produce fairly clean solitary waves. Experiments were run for a solitary wave of initial height $H = 0.1$ m in initial depth $h_1 = 0.74$ m, which gives $H/h_1 = 0.211$ (Fig. 5). Experimental data include wave elevation measured at 6 wave gages (S1-S6), visualizations of breaking wave shapes around the location of the shallower gage (S6), and flow velocities measured within the breaking wave area, using a Particle Image Velocimetry (PIV) method.

In VOF simulations, we use a $1:15$ constant slope. Calculations are made in a domain 16 meters long ($x \in [-0, 16]$) and 1.4 meters high ($y \in [-0.74, 0.3]$). The initial solution is computed with the BEM model. The exact tank geometry, wavemaker shape, and motion were specified in the BEM model, and computations were started from still water. Details can be found in Grilli et al. (2004). Incident solitary waves, to be specified in the VOF-NS model, were selected at two different times $t = 6.99$ s and $t = 8.75$ s in the BEM model, for which waves crests were located at $x = 10$ and 13.9 m, respectively. These waves are hereby referred to as I2 and I3 (Fig. 5). Internal velocity and pressure were computed for these waves in the BEM model, and used to initialize VOF-NS model computations. The computational cells used in the VOF-NS model were 2076×120 for I3 and 2160×120 for I2.

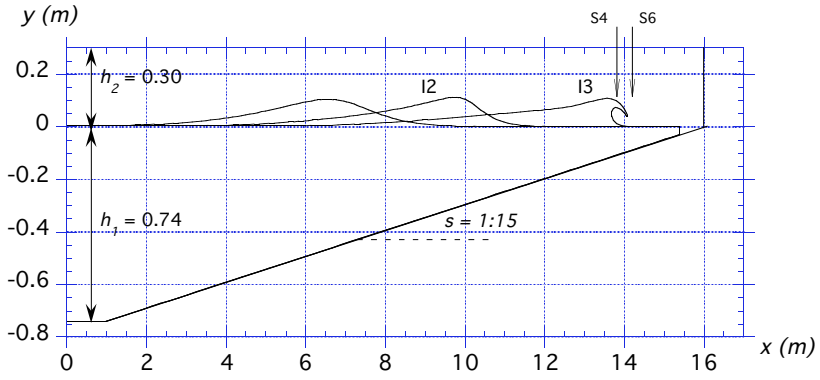

Fig. 5. Configuration of ESIM's experiments for solitary wave shoaling and breaking, with gages located at x= 13.85 (S4) and 14.20 m (S6).

Figure 6 shows the comparison of measured breaker shapes, with numerical wave profiles,

for the two different initial waves, I2 and I3. With initial solution I3, computed wave profiles are in good agreement with experiments, although wave elevations are slightly higher in the numerical model than in experiments. The BEM solution on which these VOF computations are based, in fact, also shows similar slightly higher elevations than in experiments (Fig. 7). Grilli et al. (2004) give several sources of experimental errors that can help explain these discrepancies, the principal one being the paddle motion, which was poorly controlled in experiments and hence quite difficult to reproduce exactly in the BEM model. Another source of errors is seiching in the tank during experiments.

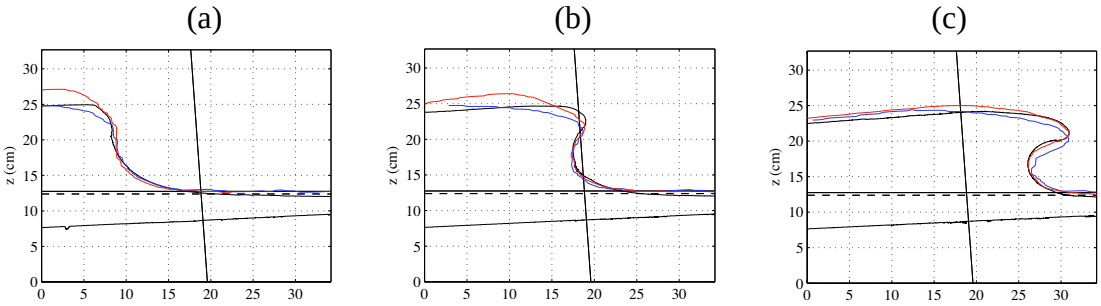

Fig. 6. Comparison of measured breaker shapes (black line) with numerical simulations, with I2 (blue line), and I3 (red line), at three different times.

With initial solution I2, wave profiles are also well computed in Fig. 6, as compared to experimental results. Here, however, the amplitude of the computed wave is slightly lower than in experiments. Wave I2 is initialized further down the slope than I3, at $x = 10$ m, and thus propagates over more than 4 m, which causes some numerical dissipation in the VOF-NS model, leading to a gradual decrease in wave amplitude during propagation. The difference between VOF-NS results and experiments is about -2.5 % at wave gage S4 and -10 % at gage S6 (Fig. 7). This loss of energy does not really affect the location where jet impact occurs in the VOF-NS model. With the initial solution I3, the breaking jet impacts the free surface at $x = 14.68$ m, and at $x = 14.72$ m with I2. In experiments, jet impact occurs between 14.50 and 14.55 m.

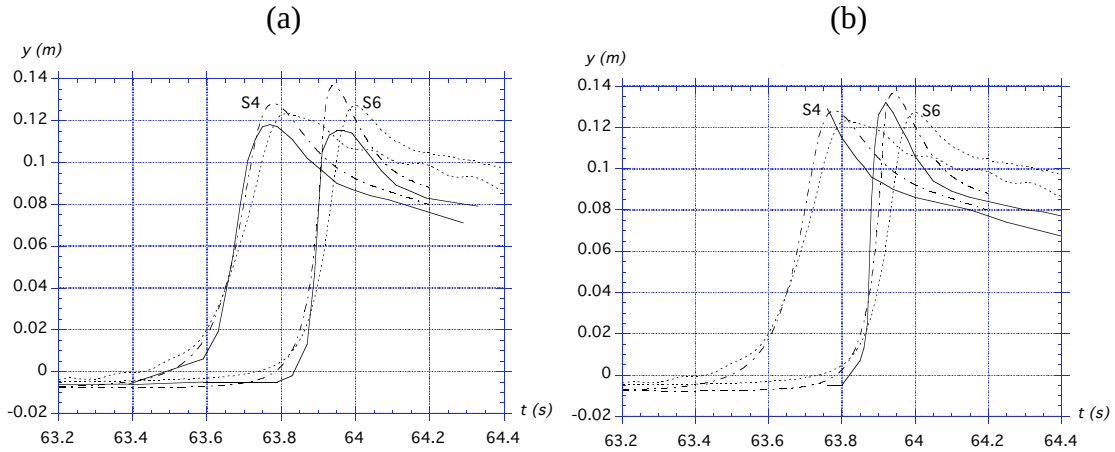

Fig. 7. Comparison of VOF-NS (——) and BEM (— - —) results with ESIM's experimental data (- - - -), for initial solutions : I2 (a); I3 (b), at wave gages: S4 and S6.

CONCLUSIONS

The validity of the coupled BEM-VOF-NS model to simulate complex wave propagation and breaking events has been tested by comparing results to experiments for the shoaling, breaking, and post-breaking of solitary waves. Two different applications were selected, corresponding to a step and a 1:15 slope.

The coupled model produces satisfactory numerical simulations of these two physical wave experiments, with a good agreement of numerical results with experiments, for both wave elevations and breaking wave profiles. However, when using an initial BEM solution that is located too far from the breaking point in the VOF-NS model, which implies long propagation/shoaling distances for the solitary wave, a measurable loss of amplitude occurs. The coupling of the two models, BEM and VOF-NS, significantly reduces or even eliminates this type of problem.

In addition to the work presented here, further results supporting these conclusions will be presented during the conference, such as the comparison of internal velocities simulated in the VOF-NS model and measured in ESIM's experiments using the PIV method. Moreover, as part of the PATOM program, other VOF-NS models were used to simulate the same experimental cases, and results of these models will be compared with our results in work that will also be reported on during the conference.

ACKNOWLEDGEMENTS

Financial support of the French CNRS PATOM program is gratefully acknowledged.

REFERENCES

Biausser B., S.T. Grilli, Fraunié P. and Marcer, R. (2004a). "Numerical analysis of the internal kinematics and dynamics of three-dimensional breaking waves on slopes." *Intl. J. Offshore and Polar Engng.*, 14(4), 247-256.

Biausser B., Guignard, S., Marcer R., and Fraunié, P. (2004b). "3D two phase flows numerical simulations by SL-VOF method." *Int. J. Numerical Methods in Fluids*, 45, 581-604.

De Jouëtte, C., Viviand, H., Wormon, S., and Gouez, J.L. (1991). "Pseudo compressibility method for incompressible flow calculation." *4th Int. Symposium on computational Fluid Dynamics*, California, Davis.

Grilli, S.T. and Horrillo, J. (1997). "Numerical Generation and Absorption of Fully Nonlinear Periodic Waves." *J. Engineering Mech.*, 123(10), 1060-1069.

Grilli, S.T., Losada, M.A.and Martin F. (1992). "The Breaking of a Solitary Wave over a Step : Modeling and Experiments." In *Proc. 4th Intl. Conf. on Hydraulic Engineering Software* (HYDROSOFT92, Valencia, Spain, July 92; eds. W.R. Blain and E. Cabrera), 575-586.

Grilli, S.T., Losada, M.A. and Martin, F. (1994). "Characteristics of Solitary Wave Breaking Induced by Breakwaters." *J. Waterway Port Coastal and Ocean Engng.*, 120(1), 74-92.

Grilli, S.T. and Subramanya, R. (1996). "Numerical modeling of wave breaking induced by fixed or moving boundaries." *Computational Mech.*, 17, 374-391.

Grilli, S.T. (1997). "Fully nonlinear potential flow models used for long wave runup prediction.", Chapter in *Long-wave runup models*, (eds. Yeh, H., Liu, p. and Synolakis, C.), World Scientific Pub, 102-112.

Grilli, S.T., Svendsen, I.A. and Subramanya, R. (1997). "Breaking Criterion and Characteristics for Solitary Waves on Slopes." *J. Waterway Port Coastal and Ocean engng.*, 123(3), 102-112.

Grilli, S.T., Gilbert, R., Lubin, P., Vincent , S., Legendre, D., Duvam, M., Kimmoun, O., Branger, H., Devrard, D., Fraunié, and P., Abadie, S. (2004). "Numerical modeling and experiments for solitary wave shoaling and breaking over a sloping beach." In *Proc. 14th Offshore and Polar Engng. Conf.* (ISOPE04, Toulon, France, May 2004), 306-312.

Guignard, S., Grilli, S.T., Marcer, R. and Rey, V. (1999). "Computation of shoaling and breaking waves in nearshore areas by the coupling of BEM and VOF methods." In *Proc. 9th Offshore and Polar Engng. Conf.* (ISOPE99, Brest, France, May 1999), III, 304-309.

Guignard, S., Marcer, R., Rey, V., Kharif, C., and Fraunié, P. (2001). "Solitary wave breaking on sloping beaches: 2D two phase flow numerical simulation by SL-VOF method." *European Journal of Mechanics B-Fluids*, 20, 57-74.

Helluy Ph., Golay F., Caltagirone J.-P., Lubin P. , Vincent S., Drevard D., Marcer R., Seguin N., Grilli S., Lesage A.-C. and Dervieux A. (2005). "Numerical simulations of wave breaking." *Math. Modeling and Numer. Analys.* (accepted).

Hirt, C., and Nichols, B. (1981). "Volume of fluid method for the dynamics of free boundaries." *J. Comp. Phys.*, 39, 323-345.

Kimmoun, O., Branger, H., and Zuchinni, B. (2004). "Laboratory PIV measurements of wave breaking on a beach." In *Proc. 14th Offshore and Polar Engng. Conf.* (ISOPE04, Toulon, France, May 2004).

Lachaume, C., Biausser, B., Grilli, S.T., Fraunié, P. and Guignard, S. (2003). "Modeling of breaking and post-breaking waves on slopes by coupling of BEM and VOF methods." In *Proc. 13th Offshore and Polar Engng. Conf.* (ISOPE03, Honolulu, USA, May 2003), 353-359.

Longuet-Higgins, M.S. and Cokelet, E.D. (1976). "The deformation of steep surface waves on water I. A numerical method of computation." *Proc. R. Soc. London*, Ser. A, 350, 1-26.

Longuet-Higgins, M.S. and Cokelet, E.D. (1978). "The deformation of steep surface waves on water II. Growth of normal-mode instabilities." *Proc. R. Soc. London*, Ser. A,364, 1-28.

Tanaka, M. (1986). "The stability of solitary waves." *Phys. Fluids*, 29(3), 650-655.

Viviand, H. (1980). "Pseudo-unsteady methods for transonic flow computations." *Int. Conf. on Numerical Methods in Fluid Dynamics, Stanford*, 141, Springer-Verlag, New-York.

Viviand, H. (1995). "Analysis of pseudo-compressibility systems for compressible and incompressible flows." *Comp. fluid Dynamics Review, Hafez-Oshima editor, Wiley publishers*, 399-418.

Yasuda, T., Mutsuda, H. and Mizutani, N. (1997). "Kinematics of overturning solitary waves and their relations to breaker types." *Coastal Engng.*, 29, 317-346.